NASA Technical Memorandum 102270

Numerical Simulation of Flow Through Two Biofluid Devices

Stuart E. Rogers and Dochan Kwak, Ames Research Center, Moffett Field, California
Cetin Kiris and I-Dee Chang, Stanford University, Stanford, California

March 1990

National Aeronautics and
Space Administration

Ames Research Center
Moffett Field, California 94035-1000

NUMERICAL SIMULATION OF FLOW THROUGH TWO BIOFLUID DEVICES

Stuart E. Rogers and Dochan Kwak
NASA Ames Research Center, Moffett Field, CA

Cetin Kiris and I-Dee Chang
Stanford University, Stanford, CA

SUMMARY

The results of a numerical simulation of flow through an artificial heart and through an artificial tilting-disk heart valve are presented. The simulation involves solving the incompressible Navier-Stokes equations; the solution process is described. The details and difficulties of modeling these geometries are discussed. The artificial heart involves a piston-type action with a moving solid wall. A single H grid is fitted inside the heart chamber. The grid is continuously compressed and expanded (the number of grid points remains constant) to accommodate the moving piston. The valve geometry involves a tilting disk inside a cylindrical chamber. An overlaid-grid approach is used to simulate this geometry. The equations must be solved iteratively for each discrete time step of the computations, thus a significant amount of computing time is required. Approximately four hours on a supercomputer are needed for one period of the artificial heart's piston motion. It is particularly difficult to analyze and illustrate the fluid physics represented by these calculations because of the time-varying nature of the flow, and because the flows are internal. Three-dimensional graphics and scientific visualization techniques have become instrumental in solving these problems.

INTRODUCTION

The science of computational fluid dynamics (CFD) uses computers to numerically solve the governing equations of fluid dynamics. CFD has grown to become a very powerful tool for studying fluid dynamics, and has been used primarily for problems in aerodynamics. Advances in CFD along with advances in supercomputer hardware have made it possible to simulate increasingly complex problems. This paper describes an effort to simulate the flow inside the chamber of an artificial heart and through an artificial heart valve. The goal of the work was to apply a CFD computer code to problems in biofluid mechanics as a demonstration of its capability to impact a broader area than just aerodynamics. Developing this capability will extend the use of CFD as a design tool into all aspects of fluid dynamic mechanisms. The analysis of blood flow through the heart, blood vessels, and various biomedical prosthetic devices requires detailed knowledge of the flow quantities. Blood may exhibit significant non-Newtonian characteristics locally, and the geometry of the biofluid mechanism is usually complicated. Also, the flow is unsteady, possibly periodic, highly viscous, and incompressible. The problems are interdisciplinary and an attempt for a complete simulation would at present be nearly impossible. However,

an analysis based on a simplified model may provide much-needed physical insight into the blood-flow analysis. More comprehensive studies on blood flow are described in references 1-5.

Various types of prosthetic heart valves have been used to replace natural valves. Currently, mechanical hearts and heart assist devices are not often used, but they are in demand as temporary life support systems. Both of these devices have several shortcomings, some of which are directly attributable to the fluid dynamics of the blood. These shortcomings include large pressure losses across the valves, which prevent the heart from working efficiently; separated flow and recirculating regions, which can lead to clotting; and high turbulent shear stress, which can damage the red blood cells. It is therefore of considerable benefit to medical researchers to be able to determine the flow characteristics in these devices by applying state-of-the-art CFD technology. Ongoing work by the authors has included the development of viscous, incompressible flow solvers. This research is motivated by the need for realistic three-dimensional (3-D) simulations in aerospace applications, such as the flow of liquid fuel through the Space Shuttle main-engine power head.

The present numerical simulation of blood flow through an artificial heart is believed to be a unique undertaking. There has been some work involving the simulation of flow through a model of an actual heart (see ref. 6). Previous numerical studies have modeled the steady-state flow through artificial heart valves in the fully open position. Underwood and Mueller (refs. 7 and 8) obtained the flow characteristics for a Kay–Shiley disk type valve. Their results showed agreement with experimental data for Reynolds numbers up to 600. Idelson et al. (ref. 9) modeled the flow through Kay–Shiley caged disk, Starr–Edwards caged ball, and Bjork–Shiley tilting disk valves, and compared their performance. A maximum Reynolds number of 1500 was reached in their numerical study. In the above studies, the caged disk and caged ball geometries were assumed to be axisymmetric, and the tilting disk geometry was simplified to two dimensions. In reality the geometries are 3-D, the flow is unsteady, and the Reynolds numbers are as high as 6500. The current work with an artificial heart valve involves a computational study of 3-D steady-state and unsteady flow through the Bjork–Shiley tilting disk at Reynolds numbers from 2390 to 6400.

The simulation of flow through these devices is computationally expensive. The elliptic nature of the incompressible flow equations requires an iterative method of solution in order to get a time history of the flow. Obtaining accurate flow solutions for geometries of this complexity requires that a large number of discrete points (on the order of 100,000) be used to define the computational grid. The quantities that define the flow field (for incompressible flow) are the three velocity components and the pressure. The result of the numerical calculations is a value for each of these quantities at each of the discrete points in the grid. If a solution is obtained for 100 discrete points in time (which may only represent a small interval of the total timespan of interest), it requires on the order of 10^8 words of disk storage. This includes the storage of the physical coordinates of the grid points which must be saved when the geometry varies with time. The code requires approximately 10^{-3} CPU sec per grid point per physical time step on a Cray 2 supercomputer, and about 3 hr for the simulation of one time interval.

The primary purpose of the current work is to apply NASA-developed technology

to research on this type of hardware. NASA benefits from advancements in CFD for treating unsteady internal flow with moving boundaries, whereas the manufacturers of biofluid devices benefit by gaining a better understanding of the fluid flow within the devices and, presumably, an improved design. In the following sections a brief description of the flow solver algorithm is given, followed by a description of the geometry definition and grid generation. Then the results of the computations are presented.

This work is part of a joint effort with Pennsylvania State University and Stanford University and is partially funded by the NASA Technology Utilization office.

COMPUTATIONAL SOLUTION METHOD

Recent developments in the numerical solution of the incompressible Navier-Stokes equations include an algorithm for time-dependent flows (refs. 10 and 11). This algorithm was implemented in a computer code called INS3D-UP, and was used for all of the calculations presented in this paper. The code solves the equations governing the flow of a constant-density, viscous fluid. A generalized curvilinear coordinate system is used which allows the use of a body-fitted grid, making it possible to readily solve for the flow over many varied shapes. The governing equations are elliptic, and, correspondingly, the speed of sound in the fluid is infinite. This means that information must be propagated from one region of the flow field to all other points in the field in the interval of one discrete physical time step. Therefore, some type of iterative technique must be used when the flow quantities are updated from one time step to the next. The approach taken by the current computer code is the method of artificial compressibility. This is implemented by introducing a pseudotime derivative of pressure to the continuity equation, which is otherwise a statement that the divergence of velocity must be zero. By performing subiterations of this equation coupled with the momentum equations, the divergence of velocity is driven to zero as the subiterations converge. The concept is straightforward: suppose that in one grid cell there is a net flux of mass leaving the cell, so the divergence of velocity is positive. There is then a drop in pressure during the next subiteration, which through the momentum equations will generate a force tending to pull the fluid back into the cell, driving the divergence of velocity toward zero.

The resulting equations are solved as follows. The convective fluxes are discretized using an upwind-differencing scheme known as flux-difference splitting. This is based on Roe's scheme (ref. 12) and is third-order accurate in space. The upwind scheme has several advantages over the simpler and more traditional central-difference approaches. First, the system of numerical equations resulting from the upwind scheme is more nearly diagonally dominant than that resulting from the use of a central-difference scheme. This diagonal dominance leads to fast convergence in the subiterations. Second, the upwind approach does not require the user to specify artificial dissipation coefficients, which would be needed to stabilize nonlinear oscillations accompanying a central-difference scheme. The viscous fluxes are discretized using second-order central differencing, thus the overall spatial accuracy is second order. The time integration is second-order accurate. Once the numerical equations are formed they are solved using an unfactored, implicit, line-relaxation algorithm which has proved to have good stability and convergence character-

istics. The boundary conditions used with this flow solver are implicit and nonreflective at the inflow/outflow boundaries.

GEOMETRY AND GRID GENERATION

In this section the geometry definition and grid generation for the two different devices are discussed. Both devices present a challenge, as they both have moving parts and unusual shapes. There are two basic approaches to developing a grid which is fitted to all parts of the body, both moving and stationary. In the first approach, a single grid is used and is allowed to move to conform to the motion of the surfaces. A second method, known as the Chimera grid embedding technique (refs. 13 and 14), uses a number of overlaid grids superimposed on each other. This technique allows one grid to be placed around a moving surface, and another to be used for the stationary part of the body; thus the grids move relative to each other. Information is passed between the boundaries of the overlapping grids by interpolating the flow quantities from one grid and then specifying these values as boundary conditions on the other. Although this leads to more overhead in the computation, it makes the grid generation simpler.

Artificial Heart

A computer-generated shaded-surface representation of an artificial heart developed at Pennsylvania State University is shown in figure 1. The heart is composed of a cylindrical chamber with two openings on the side for valves. The pumping action is provided by a piston surface which moves up and down inside the chamber. A tube extends out of each of the valve openings. The tubes contain tilting flat disks which act as the valves. The current computational model neglects the valves altogether and uses the right and left openings for the inflow and outflow boundaries, respectively. In the computations, as the piston reaches its top-most position, the outflow valve closes and the inflow valve opens instantaneously. Similarly, as the piston reaches its bottom-most position, the outflow valve opens and the inflow valve closes.

In the actual heart device, the piston moves through the entire chamber, across most of the valve opening. This first attempt at computing the flow uses a single grid, with a constant number of grid points, which expands and contracts with the motion of the piston. A new grid is generated for each time step during the running of the code. For the implementation of the boundary conditions at a valve opening, it is necessary to place the grid lines around the valve to coincide with the valve opening boundaries. Yet because the piston moves past this opening, the grid has to accommodate both surfaces. It is very difficult to generate a grid without any grid lines crossing over each other. A satisfactory grid has not been obtained for the point in time when the piston moves past the bottom of the openings for the valves. The current computation therefore restricts the motion of the piston such that it stays below the valve openings.

To make the most efficient use of grid points, an H-H grid topology was used to fit the grid to the physical domain. Because of computational time limitations of the flow solver, the grid dimensions were chosen to be $39 \times 39 \times 51$ grid points. In order to

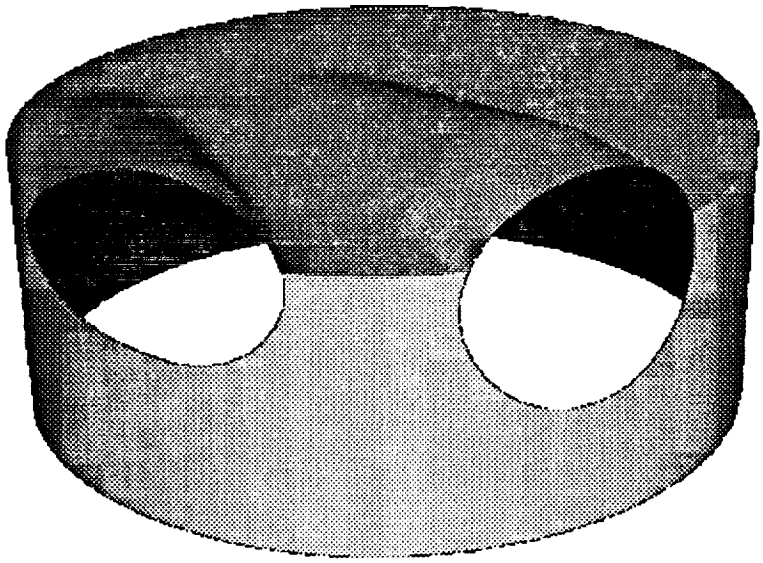

Figure 1. Artificial heart geometry showing valve openings.

generate a grid at each time step for this geometry, the surface grid was first generated, and an algebraic grid generator and elliptic smoother were used to generate the interior points using the distribution given on the surface grid. To generate the surface grid the side boundary was divided into seven zones. The points were distributed along each of the zonal boundaries, and then a biharmonic solver written by Bjorstad (ref. 15) was used to generate the grid interior to each of the surface zones. The biharmonic solver was also used to generate an H grid for the top and bottom surfaces of the heart device. This approach made it relatively simple to repeat the process at each time step for any position of the piston surface. Figure 2 shows the unwrapped surface grid on the side of the heart chamber.

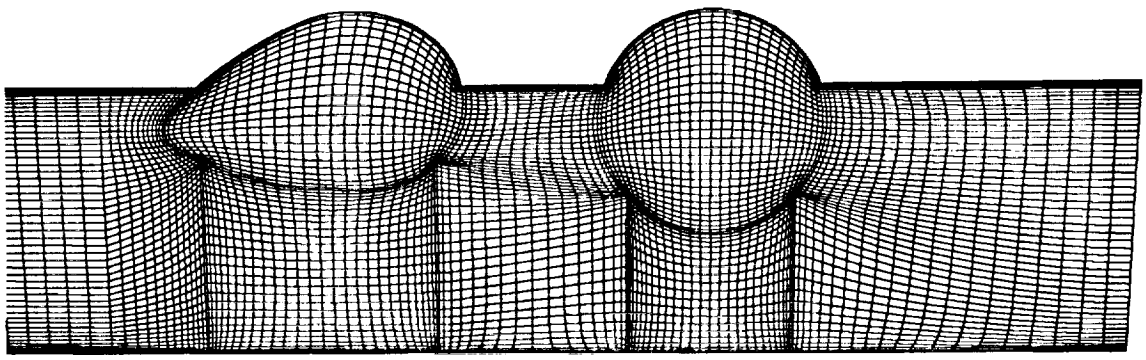

Figure 2. Unwrapped side surface of the artificial heart.

Tilting-Disk Valve

The computational geometry for the Bjork–Shiley tilting-disk heart valve is shown in figure 3. The disk motion is illustrated by showing three different positions of the disk. The disk angles shown are 75°, 50°, and 30°, as measured from the centerline of the aorta. The disk rotates about an axis which is one-sixth of a disk diameter below the center of the disk. The inflow conditions are symmetric, allowing an assumption of overall bilateral symmetry.

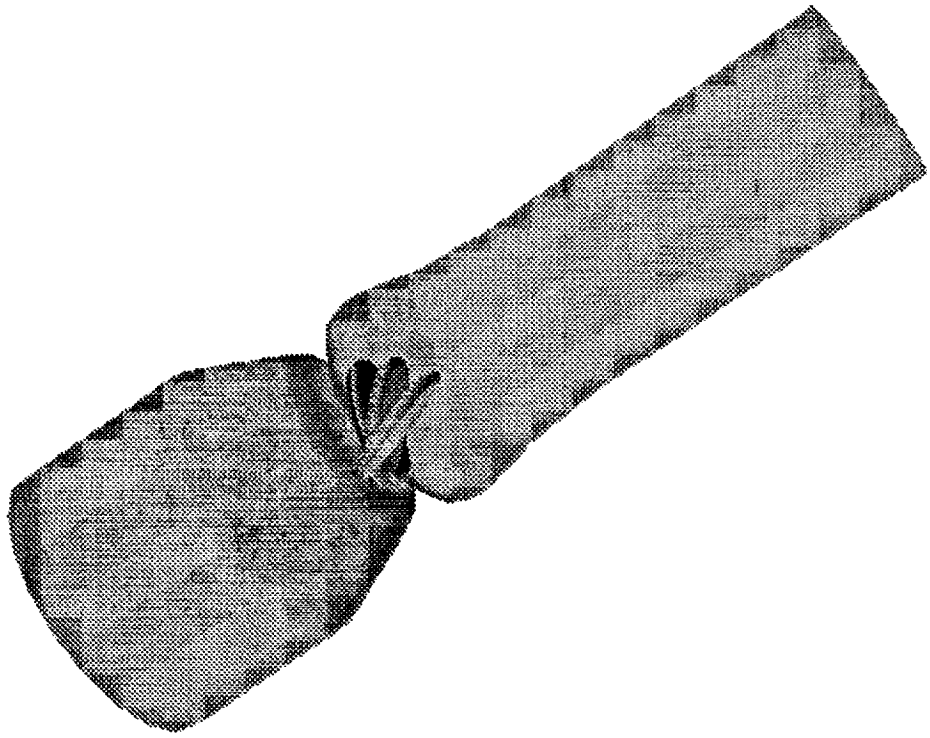

Figure 3. Geometry of the prosthetic tilting-disk valve.

The only way to model this geometry with an ordered grid is to use a multizonal approach. Since there are moving parts, the chimera grid embedding technique is a straightforward method to use. Two overlapped grids are used, as shown in figure 4. Grid 1 occupies the entire region of the aorta, from entrance to exit, and always remains stationary; grid 2 wraps around the tilting disk and moves with the disk. Points from grid 2 that lie outside the aorta grid are excluded from the solution process. The excluded points are called hole points, and the points next to the hole points are called fringe points. The information is passed from one grid to another via fringe points by interpolating the dependent variables.

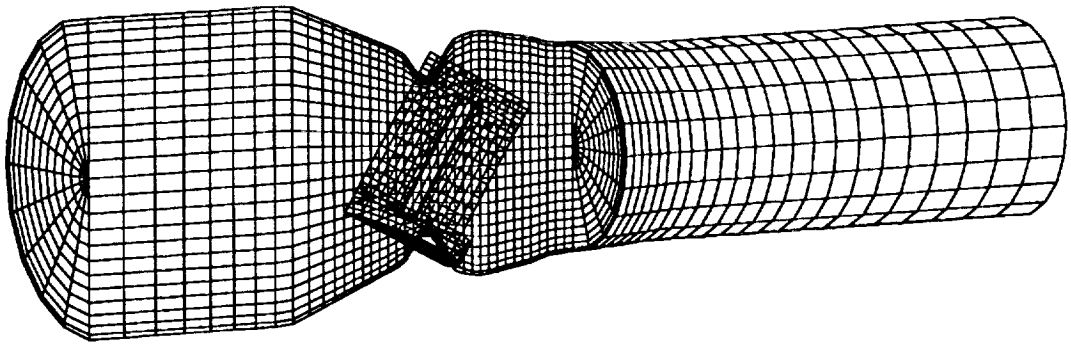

Figure 4. Overlaid grids used for the prosthetic tilting-disk valve.

COMPUTED RESULTS

The calculations for the artificial heart chamber were done on a Cray 2 supercomputer, and the calculations for the valve were done on a Cray XMP.

Artificial Heart Computations

The computations were initialized with the fluid at rest, with the piston at the bottom position and the outflow valve open. The computations were carried out for a Reynolds number of 100 based on unit length and velocity, and the flow was assumed to be laminar. In the actual artificial heart the Reynolds number is about 600, and regions of the flow are turbulent. The laminar assumption was used here because the main purpose of this calculation was to test the ability of the flow solver to compute flow through this complicated geometry, separate from the effects of using the turbulence model. Finally, the fluid was assumed to be Newtonian, as in the experiment of Tarbell et al. (ref. 4), in which a water-and-glycerin fluid with viscosity nearly the same as blood (about 3.5 centipoise) was used. Unlike blood, the glycerin mixture exhibits a Newtonian fluid behavior.

The physical time step, Δt, was set to 0.025. Larger values of Δt tended to make the computation unstable. The piston moved with a constant non-dimensionalized velocity of ± 0.2 between its top and bottom positions, thus 200 physical time steps were required for one period of the piston's motion. During each time step, the subiterations were carried out until the maximum residual dropped below 10^{-3} or until a maximum of 20 subiterations were done. During most of the piston's cycle only 12-15 subiterations were required, but when the piston was changing direction, complete convergence was not achieved in 20 subiterations. This did not cause any stability problems, yet it remains to be seen what effect it had on the accuracy of the solution. The computing time required for each period of the piston's motion was approximately 4 hr. The computations were run for four periods, during which the particle paths were computed after the particles were released near the inflow valve.

Once the computations are completed, the results must be interpreted for an understanding of the fluid physics involved. Since the flow is time dependent, a lot of data are produced, and the problem is essentially four-dimensional. It is difficult to show the

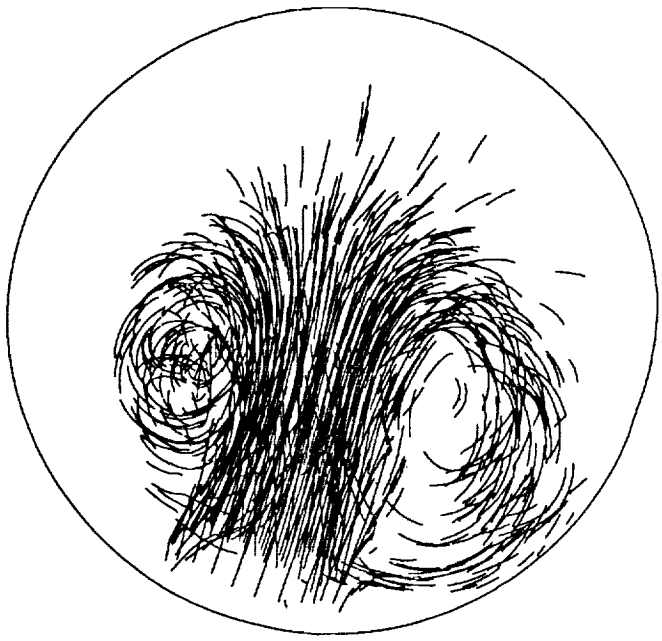

(a) Computational results.

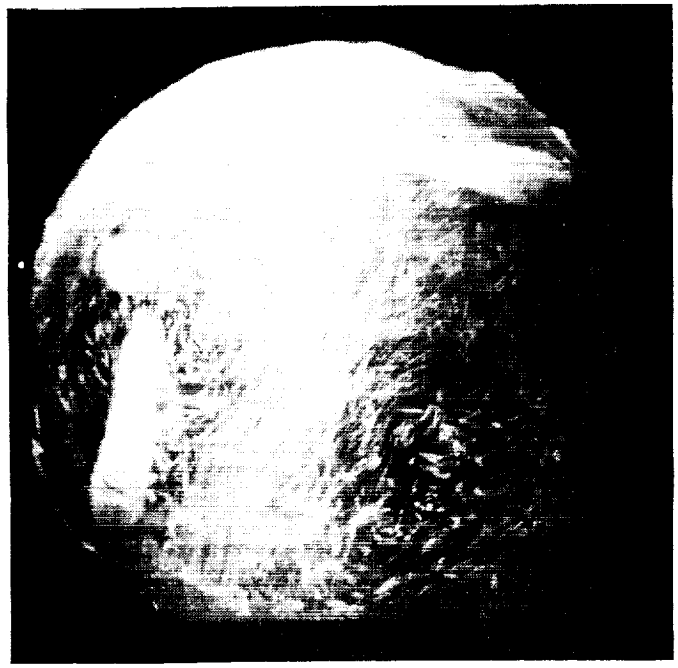

(b) Experimental results.

Figure 5. Incoming particle traces from computations, and photograph of experimental results, as the piston nears the bottom position.

physics of the fluid using two-dimensional media. There are several methods of presenting the data, including drawing color contours of scalar variables such as pressure, and drawing vectors of data such as velocity. One of the best methods is to plot particle traces. This is done by integrating the velocity field in time to produce lines which show the path traveled by a series of fluid particles. This method can give a fairly complete visualization when the lines are animated on a computer. In addition, the color of a particle trace can vary along its path in proportion to some scalar variable of interest, adding more information about the flow field.

Figure 5(a) shows some of the particle traces as the piston nears its bottom position. Two distinct vortices have formed from the flow separating as it enters through the inflow valve and encounters the lower pressure regions near the valve. In figure 5(b), an experimental photograph (J. M. Tarbell, personal communication) shows bubbles entering the inflow valve as the piston nears its bottom position. A similar two-vortex system is seen here.

Valve Computations

The geometry used in these calculations is similar to that used in the experimental studies of Yoganathan, et al. (refs. 16 and 17) (steady-state) and of Figliola and Mueller (ref. 18) (unsteady). The inflow and outflow boundaries for the calculations were specified to be a shorter distance from the valve than they were in these experiments. This reduced the computational requirements for the problem. The exact shape of the sinus region of the aorta used in the experiments is not known. These discrepancies could lead to slight differences between the computational results and the experimental data. The Reynolds numbers used in the calculations are based on the disk diameter and the mean velocity at the entrance of the channel. The physiological range of Reynolds numbers for these problems is in a regime where turbulence will be important. The computations use an algebraic mixing-length turbulence model to compute a turbulent viscosity which models the turbulence effects.

Steady-State Computations.– Steady-state calculations were carried out with the disk at 30° and with Reynolds numbers ranging from 2000 to 6000. Figure 6 shows the pressure drop across the valve at different flow rates of physiological interest, from the computations and from the experimental results of Yoganathan et al. (refs. 16 and 17). There is good agreement between the two. In figure 7, the axial velocity profile downstream of the disk in the horizontal plane through the center of the channel is plotted for both the computations and the experiment, for a Reynolds number of 5972. Again, there is fairly good agreement. The largest discrepancy is seen near the walls, where the boundary-layer thickness is overestimated by the calculation. This is most likely a result of inaccuracies of the turbulence modeling. Figure 8 shows velocity vectors in the lateral plane of symmetry, also for a Reynolds number of 5972. The recirculation region in the sinus area of the aorta, and a large separated region along the lower wall of the aorta, can be seen.

Unsteady Computations.– The computations of the unsteady flow begin with the disk closed and the fluid at rest. The flow is started by specifying velocity at the inflow boundary, and the disk starts to rotate open. The Reynolds number is 6400. Figure 9

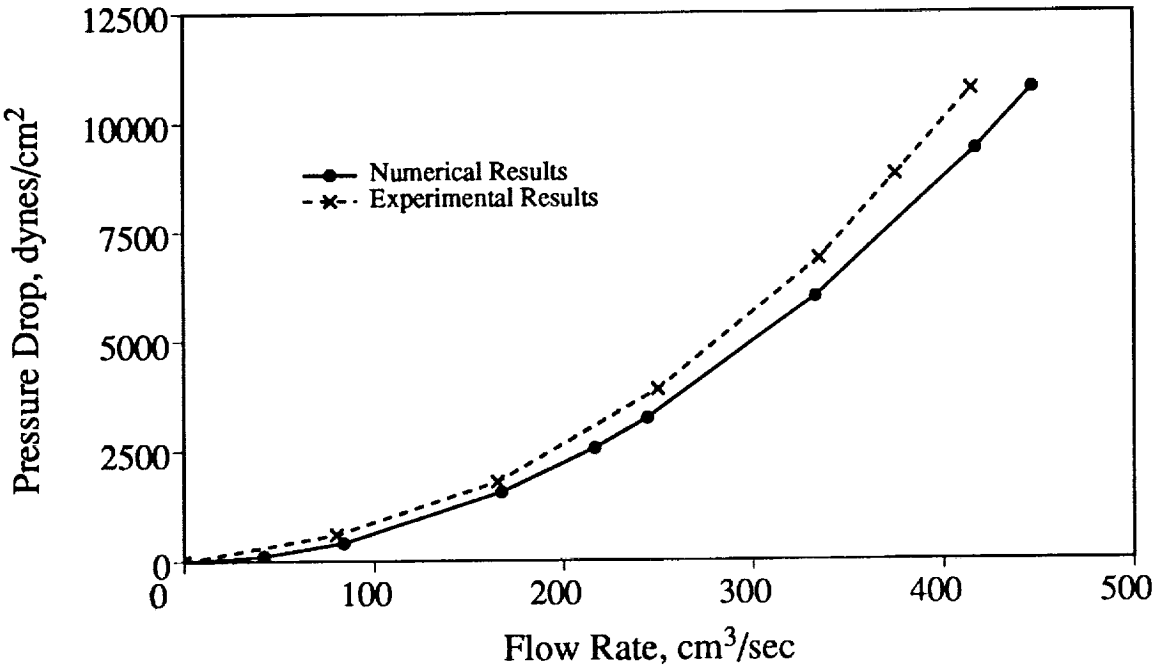

Figure 6. Steady-state pressure drop across the Bjork–Shiley valve.

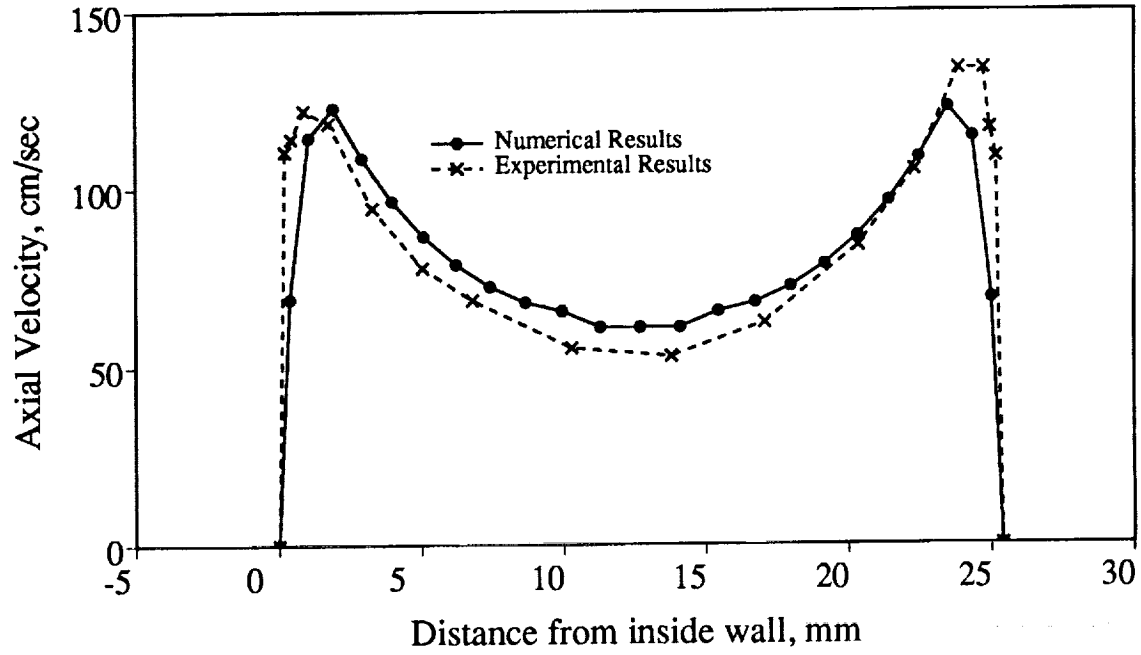

Figure 7. Axial velocity profile downstream of the disk in the horizontal plane through the center of the channel, Re = 5972.

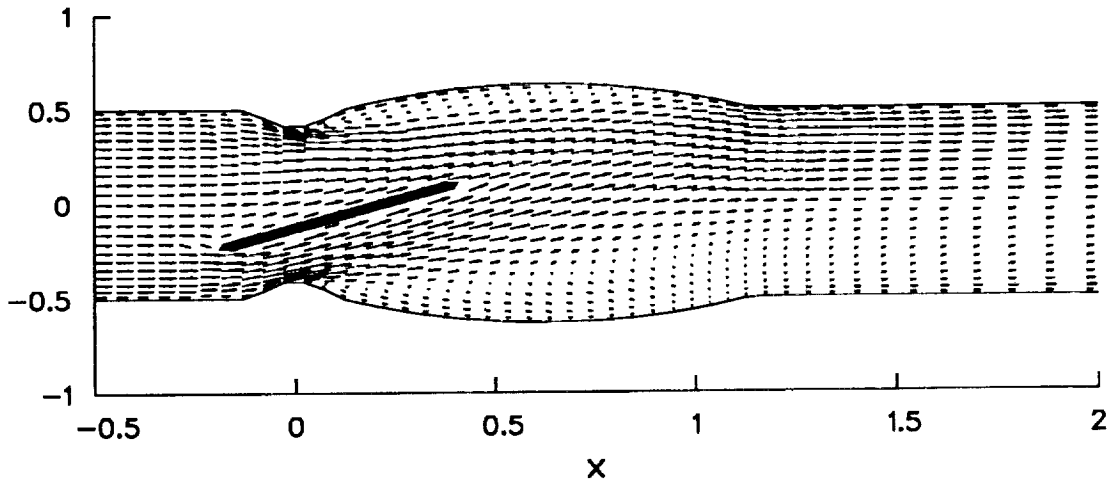

Figure 8. Velocity vectors in the lateral plane of symmetry for the steady-state case at Re = 5972.

shows the velocity vectors in the lateral plane of symmetry. The three plots illustrate the flow for disk angles of 75°, 45°, and 20°. The separation region along the lower wall of the aorta is compressed as the disk rotates to its open position. When the disk begins to open, the flow starts to separate behind the disk, and it reattaches to the wall. The vortices in the sinus region of the aorta grow during this process.

Figliola and Mueller (ref. 18) experimentally measured the velocity near the top and bottom walls, and computed the shear stress. The maximum shear was observed to occur at the top wall just downstream of the sinus region of the aorta. This is in agreement with the velocity plots shown in figure 9, in which there are large velocity components just off the wall in that location. This phenomenon is particularly evident when the valve starts to open, as can be seen in the first plot in figure 9.

CONCLUSIONS

An algorithm for computing unsteady incompressible Navier-Stokes equations has been extended to simulate the flow through an artificial heart and past a tilting-disk heart valve. The solution shows the capability of the computational procedure for simulating complicated internal flows with moving boundaries. The calculations require a significant amount of computing time on a supercomputer, but the potential payoff in understanding the complex flow physics inside these devices is large. Several simplifying assumptions were made for the artificial heart calculation, such as the restricted piston motion and the low Reynolds number. However, the success of the subsequent valve calculations shows that this weakness can be overcome. The use of the chimera overlap-grid strategy will make it possible to move the piston through the entire chamber without causing grid generation problems. The turbulence model used in the valve calculations will enable the use of more realistic Reynolds numbers. Work is under way to calculate the flow through an entire artificial heart, complete with inflow and outflow tilting disk valves.

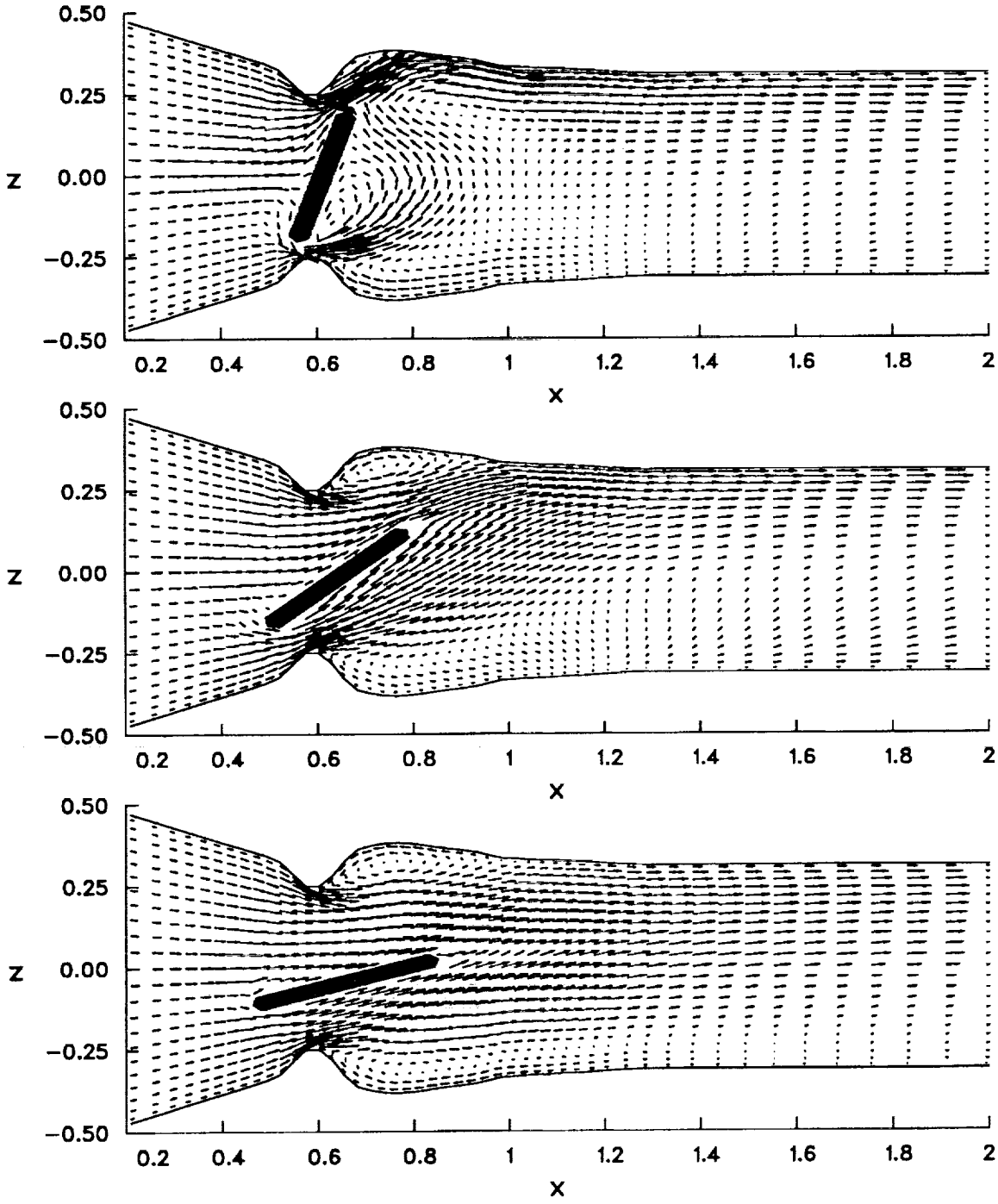

Figure 9. Velocity vectors showing valve opening at disk angles of 75° (top), 45° (middle), and 20° (bottom).

The next step will be to reduce the turn-around time needed for a computational solution. Since it takes 10-20 hr of computer time to simulate the pumping of an artificial heart complete with valves, and because supercomputers often have long queues, the current turn-around time for detailed flow information is often many days. Improvements both in algorithm efficiency and in computational speed of the computers are needed.

REFERENCES

1. Tiderman, W. G.; Steinle, M. J.; and Phillips, W. M.: Two-Component Laser Velocimeter Measurements Downstream of Heart Valve Prostheses in Pulsatile Flow. J. Biomech. Engr., Trans. ASME, vol. 108, 1986, pp. 59–64.
2. Liepsch, D.; Moravec, S.; Rastogi, A. K.; and Vlachos, N. S.: Measurement and Calculations of Laminar Flow in a Ninety-Degree Bifurcation. J. Biomech., vol. 15, 1983, pp. 753–766.
3. Liepsch, D.; Steiger, H. J.; Poll, A.; and Reulen, H.-J.; Hemodynamics Stress in Lateral Sacular Aneurysms. J. Biorheology, vol. 24, 1987, pp. 689–710.
4. Tarbell, J. M.; Gunshinan, J. P.; Geselowitz, D. B.; Rosenburg, G.; Shung, K. K.; and Pierce, W. S.: Pulse Ultrasonic Doppler Velocity Measurements Inside a Left Ventricular Assist Device. J. Biomech. Engr., Trans. ASME, vol. 108, 1986, pp. 232–236.
5. Peskin, C. S.: The Fluid Dynamics of Heart Valves: Experimental, Theoretical and Computational Methods. Ann. Rev. Fluid Mech., vol. 14, 1982, pp. 235–259.
6. Peskin, C. S.: Numerical Analysis of Blood Flow in the Heart. J. Comp. Phys., vol. 25, 1977, pp. 220–252.
7. Underwood, F. N.; and Mueller, T. J.: Numerical Study of the Steady Axisymmetric Flow Through a Disk-Type Prosthetic Heart Valve in a Constant Diameter Chamber. J. Biomech. Engr., vol. 99, 1977, pp. 91–97.
8. Underwood, F. N.; and Mueller, T. J.: Numerical Study of the Steady Axisymmetric Flow Through a Disk-Type Prosthetic Heart Valve in an Aortic-Shaped Chamber. J. Biomech. Engr., vol. 101, 1979, pp. 198–204.
9. Idelsohn, S. R.; Costa, L. E.; and Ponso, R.: A Comparative Computational Study of Blood Flow Through Prosthetic Heart Valves Using The Finite Element Method. J. Fluid Mech., vol. 18, 1985, pp. 97–115.
10. Rogers, S. E.; and Kwak, D.: An Upwind Differencing Scheme for the Time-Accurate Incompressible Navier-Stokes Equations. AIAA Paper 88-2583, 1988.
11. Rogers, S. E.; and Kwak, D.: Numerical Solution of the Incompressible Navier-Stokes Equations for Steady-State and Time-Dependent Problems. AIAA Paper 89-0463, 1989.
12. Roe, P. L.: Approximate Riemann Solvers, Parameter Vectors, and Difference Schemes. J. Comput. Phys., vol. 43, 1981, pp. 357-372.
13. Dougherty, F. C.; Benek, J. A.; and Steger, J. L.: On Applications of Chimera Grid Schemes to Store Separation. NASA TM 88193, 1985.

14. Beneck, J. A.; Buning, P. G.; and Steger, J. L.: A 3-D Chimera Grid Embedding Technique. AIAA Paper 85-1523-CP, 1985.
15. Bjorstad, P. E.: Numerical Solution of the Biharmonic Equation. Ph.D. Dissertation, Stanford University, 1980.
16. Yoganathan, A. P.; Concoran, W. H.; and Harrison, E. E.: In Vitro Velocity Measurements in the Vicinity of Aortic Prostheses. J. Biomechanics, vol. 12, 1979, pp. 135–152.
17. Yoganathan, A. P.; Concoran, W. H.; and Harrison, E. E.: Pressure Drops Across Prosthetic Aortic Heart Valves Under Steady and Pulsatile Flow. J. Biomechanics, vol. 12, 1979, pp. 153–164.
18. Figliola, R. S.; and Mueller, T. J.: On the Hemolytic and Thrombogenic Potential Occluder Prosthetic Heart Valves from In-Vitro Measurements. J. Biomech. Engr., vol. 103, 1981, pp. 83–90.

NASA
National Aeronautics and Space Administration

Report Documentation Page

1. Report No.	2. Government Accession No.	3. Recipient's Catalog No.
NASA TM-102270		

4. Title and Subtitle	5. Report Date
Numerical Simulation of Flow Through Two Biofluid Devices	March 1990
	6. Performing Organization Code

7. Author(s)	8. Performing Organization Report No.
Stuart E. Rogers, Dochan Kwak, Cetin Kiris,* and I-Dee Chang*	A-90044
	10. Work Unit No.
*Stanford University, Stanford, CA	505-60

9. Performing Organization Name and Address	11. Contract or Grant No.
Ames Research Center Moffett Field, CA 94035-1000	
	13. Type of Report and Period Covered
12. Sponsoring Agency Name and Address	Technical Memorandum
National Aeronautics and Space Administration Washington, DC 20546-0001	14. Sponsoring Agency Code

15. Supplementary Notes

Point of Contact: Stuart E. Rogers, Ames Research Center, MS 258-1,
Moffett Field, CA 94035-1000 (415) 604-4481 or FTS 464-4481

This paper was submitted to the International Journal of Supercomputer Applications

16. Abstract

The results of a numerical simulation of flow through an artificial heart and through an artificial tilting-disk heart valve are presented. The simulation involves solving the incompressible Navier-Stokes equations; the solution process is described. The details and difficulties of modeling these geometries are discussed. The artificial heart involves a piston-type action with a moving solid wall. A single H grid is fitted inside the heart chamber. The grid is continuously compressed and expanded (the number of grid points remains constant) to accommodate the moving piston. The valve geometry involves a tilting disk inside a cylindrical chamber. An overlaid-grid approach is used to simulate this geometry. The equations must be solved iteratively for each discrete time step of the computations, thus a significant amount of computing time is required. Approximately four hours on a supercomputer are needed for one period of the artificial heart's piston motion. It is particularly difficult to analyze and illustrate the fluid physics represented by these calculations because of the time-varying nature of the flow, and because the flows are internal. Three-dimensional graphics and scientific visualization techniques have become instrumental in solving these problems.

17. Key Words (Suggested by Author(s))	18. Distribution Statement
Artificial heart Incompressible Navier-Stokes Upwind differencing	Unclassified-Unlimited Subject Category - 64

19. Security Classif. (of this report)	20. Security Classif. (of this page)	21. No. of Pages	22. Price
Unclassified	Unclassified	17	A02